Chapter 6

Superconducting Magnet Technology for the Upgrade

E. Todesco[1], G. Ambrosio[2], P. Ferracin[1], J. M. Rifflet[1], G. L. Sabbi[3], M. Segreti[4], T. Nakamoto[5], R. van Weelderen[1] and Q. Xu[5]

[1]*CERN, TE Department, Genève 23, CH-1211, Switzerland*
[2]*Fermi National Accelerator Laboratory, Batavia, IL 60510, USA*
[3]*Lawrence Berkeley National Laboratory, Berkeley, CA 94720, USA*
[4]*CEA, Saclay, 91400, France*
[5]*KEK, 1-1 Oho, Tsukuba, Ibaraki 305-0801, Japan*

In this section we present the magnet technology for the High Luminosity LHC. After a short review of the project targets and constraints, we discuss the main guidelines used to determine the technology, the field/gradients, the operational margins, and the choice of the current density for each type of magnet. Then we discuss the peculiar aspects of each class of magnet, with special emphasis on the triplet.

1. Targets

The HL-LHC aims at gathering 3,000 fb^{-1} over ten years. As discussed in the previous section, this ambitious target can be obtained by operating with a peak luminosity leveled at 5×10^{34} $cm^{-2}s^{-1}$. The plan is to obtain it through higher intensity/lower emittance and a larger focusing in the Interaction Point (IP). This second part is given by the magnetic lattice; the target is to be able to reduce the beam size in the IP by a factor two, and therefore one has to double the size of the quadrupoles aperture in front of the IP (triplet).

Some of the previous proposals, done during the LHC luminosity upgrade studies [1, 2, 3], aimed at a reduction of the beam size of 30%, increasing the triplet aperture 30% (see Fig. 1 for an historical view, indicating short models which have been built). The present target of reducing the beam size in the IP by a factor of two was based on theoretical studies (see for instance [4]), and was enabled by advances in magnet technology, i.e., test results from model quadrupoles of progressively larger aperture (Fig. 1).

A critical design parameter for a superconducting quadrupole is the peak field in the coil, which is a function of the aperture times the gradient. For Nb-Ti coils

Operated by Fermi Research Alliance, LLC under Contract No. De-AC02-07CH11359 with the United Stat

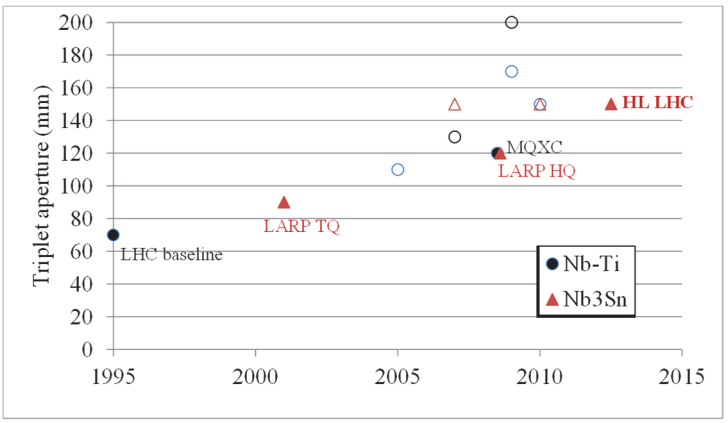

Fig. 1. Proposed aperture for the inner triplet versus time: triangles (Nb_3Sn), circles (Nb-Ti), built hardware in full markers, and proposally in empty markers.

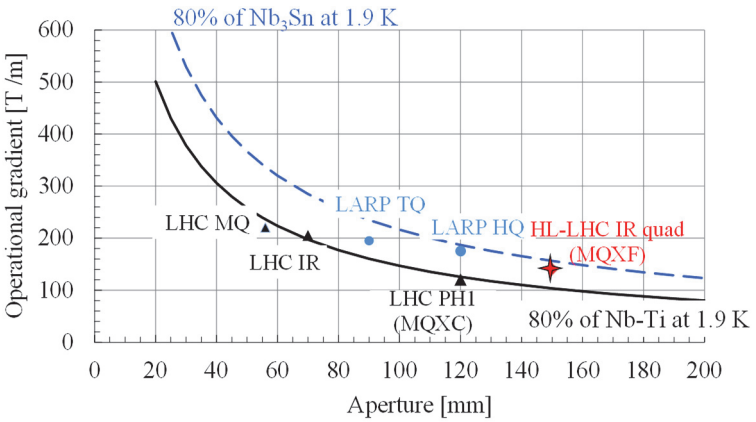

Fig. 2. Operational gradient (20% margin) versus aperture in Nb-Ti and Nb_3Sn quadrupoles.

the peak field limit in operational conditions is about 8 T [5], whereas for Nb_3Sn this limit is ~15 T. One can prove that Nb_3Sn quadrupoles give 50% more gradient w.r.t. Nb-Ti for the same aperture [6] (see Fig. 2): this allows to have shorter magnets w.r.t. Nb-Ti. As explained in the previous chapter, a compact triplet means not only more space for other components, in a critical region of the tunnel, but also (and especially) additional performance: a shorter triplet means that the beam size has less longitudinal space to grow, and therefore for the same aperture one can squeeze the beam more in the IP. Moreover, a shorter triplet allows reducing the number of long range beam–beam interactions and to reduce chromatic aberrations. So, Nb_3Sn is the enabling technology to reach the ambitious target of the HL-LHC project.

2. Constraints

2.1. *Radiation damage and heat load*

The design of the final focus system of the upgraded LHC needs to account for the special conditions related to its proximity to the interaction points. The first important constraint for the magnetic system is the radiation damage, which is proportional to the integrated luminosity. Some essential components employed for magnet fabrication (epoxy resins) undergo severe degradation at 50–100 MGy. Therefore, one needs to set a safe dose limit of 10–20 MGy or switch to radiation resistant materials, as used for nuclear fusion, which can operate in the range of 100 MGy and more. For the HL-LHC we set a target for radiation damage at 30 MGy.

The second relevant constraint for the magnetic system is the heat deposition on the coil, which is proportional to the peak luminosity. In the stationary regime of continuous heat deposition, it induces a temperature gradient between the helium bath ($T_{\text{bath}} = 1.9$ K) and the temperature of the coil $T_{\text{coil}} = (1.9 + \Delta T)$. In the LHC triplet, the limit to the heat load is given by the requirement of having superfluid helium in the coil, i.e. a temperature lower than 2.17 K, which means $\Delta T < 0.27$ K [7]. The actual design limit is set to one third of the theoretical ΔT in order to account for uncertainties in the thermal analysis or variations in the heat load and cooling conditions. For the present inner triplet quadrupoles built with Nb-Ti conductor, this corresponds to a power deposition limit of 4 mW/cm^3, with a safety factor 3. For Nb_3Sn, with the same safety factor, one can withstand 12 mW/cm^3 [8].

Simulations of energy deposition in the HL-LHC show that without any shielding one has about 200 MGy peak dose and a peak heat load of 20 mW/cm^3. This regime is not acceptable for both aspects. The peak is localized in the horizontal and vertical planes. Shielding is very effective: with a 6-mm-thick tungsten shielding, one can bring these values down by a factor five, i.e. to 40 MGy and 4 mW/cm^3 [9].

Using an additional shielding in the quadrupole Q1 close to the IP (see Fig. 3), where the aperture requirement is smaller due to a smaller size of the beam, one can further reduce these values by a factor of two. Therefore, one ends up with a radiation damage similar to what is expected for the LHC (20–25 MGy) and a lower heat load (2 mW/cm^3), see Fig. 4.

The absorbers installed in the magnet bore address two of the most significant challenges of the LHC luminosity upgrade, namely the radiation damage and the heat load. To maintain the required space for the beam the final aperture of the quadrupoles has been fixed to 150 mm, i.e. slightly more than 140 mm (the double of present triplet) that was initially required by beam dynamics.

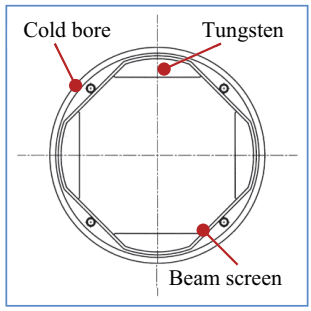

Fig. 3. Cold bore, beam screen and tungsten shielding in Q1.

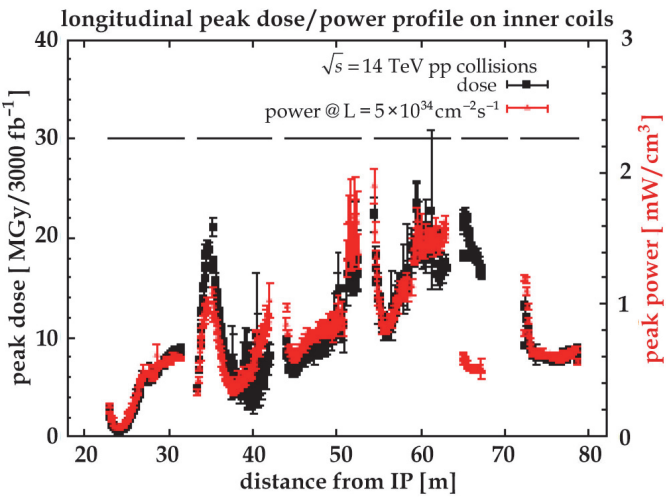

Fig. 4. Heat deposition in the coil (left scale), and radiation damage (right scale) for the 150 mm aperture triplet.

Two additional requirements point in the direction of a thick shielding as the only viable choice for the project. The total heat load on the triplet and separation dipole is 1.5 kW over 55 m, i.e. 30 W/m. The massive shielding allows to intercept about 800 W in the beam screen + shielding and remove it at intermediate temperature with higher efficiency. The remaining 700 W load needs to be removed from the cold mass at 1.9 K. This requires two heat exchangers of 70 mm diameter, barely fitting into the magnet cross-section [10]. A larger heat load would require larger heat exchangers, and larger magnet diameter, which is already at the limit of the constraints imposed by the tunnel diameter.

The second aspect is the degradation of copper Residual Resistivity Ratio (RRR) due to the radiation dose. This parameter is defined as the ratio between the resistivity at room temperature and at 1.9 K, related to the purity of copper. RRR

must be > 150 to guarantee the conductor stability and a proper protection in case of quench. Recent studies pointed out that with 200 MGy the RRR is reduced by one order of magnitude [11]. Therefore, a dose of 200 MGy would also endanger the magnet operation and its protection. This degradation is partially wiped out by a warm-up to room temperature, so one could have problems in case of very long runs without warm-up. However, with the 6-mm-thick shielding, the copper RRR degradation becomes negligible.

2.2. *Field quality*

When beams are brought in collision, the beta functions in the triplet and in the separation dipole become very large, reaching peak values of ~ 20 km, i.e. five times larger than the nominal LHC values. In these conditions, the beams become very sensitive to magnetic field errors: for this reason the field quality constraints are very tight. On the other hand, at injection the interaction region gives a small contribution to the total budget of field imperfection of the accelerator and therefore the field quality targets can be significantly relaxed. For instance the b_6 systematic component in the quadrupole at injection can be as large as 25 units (i.e. 0.25% of the main field at two/third reference radius), but must be smaller than 0.5 units at high field (see previous chapter).

The field quality optimization should therefore concentrate on high field conditions. Considering that the final energy of the LHC beams could be in the range between 6.5 TeV and at 7 TeV, the field quality must also be maintained over the corresponding operational range.

A large set of correctors magnets (up to order 6) is foreseen in the layout to be able to correct field errors and/or add nonlinearities to counter beam instabilities; in fact since the beam size is very large in the correctors, they are very effective to correct any nonlinear unwanted component of the whole LHC.

2.3. *Fringe field and magnet size*

We roughly double the magnet apertures w.r.t. the LHC baseline, but the size of the cold mass is limited by the maximum cryostat size. Today in the LHC we have a cryostat with a 980 mm diameter that is not far from the limit imposed by the tunnel transverse size.

We propose to marginally increase the cold mass size from 570 to 630 mm to partly compensate for the aperture increase, with a weight increase of less than 20%. A larger increase would be difficult since some clearance is needed between the cryostat and the magnet.

In these conditions it is unavoidable to have a large magnetic field outside the cryostat: the transverse fringe field reaches ~ 50 mT on the cryostat surface. There is no specification of the allowed field in the LHC tunnel; this value depends on the specific instrumentation *in situ* (vacuum valves, beam position monitors, beam loss monitors, quench protection equipment,…) and in some cases one can envisage a displacement or shielding of the instrument (which is less invasive than shielding the magnet). An alternative solution is an active magnetic shielding, but at the price of an increased complexity of interconnections and number of components. In this phase of the design study we set a target of 50 mT maximum field on the cryostat and we do not envisage active shielding.

3. Main Design Choices

3.1. *Foreword: Loadline, critical surface and margin*

A superconducting magnet has most of the field produced by transport current, plus a second order contribution given by the iron magnetization: therefore in a first approximation the field is proportional to the current density in the coil: the relation peak field in the coil B_p versus current density j is called the loadline.

A superconducting coil can tolerate up to a given combination of field, current density and operational temperature: this is a property of the superconductor called the critical surface (see Fig. 5). Materials that can tolerate larger values of field and current density have a better performance, allowing to reach larger fields or to make more compact coils. When the loadline crosses the critical surface, one has the maximum theoretical reachable field. It is called short sample limit since the critical surface is usually measured for a short sample of conductor (see Fig. 6).

A critical choice for magnet design is the width of its winding. The peak field is proportional to the current density and to the width of the coil, so with large coils widths, the loadline in the *B-j* graph has a lower slope and one can reach higher fields (see Fig. 6). However, a magnet with larger coil is less effective, less compact, needs more superconductor, and has lower current density w.r.t. one with smaller coil width. For larger and larger coils an asymptotic field is reached, the gain becoming more and more marginal: one needs to find the optimal coil width [12].

There are two more aspects that add to what may seem a pure cost and size problem: firstly, larger current densities imply larger mechanical stress induced by the electromagnetic forces (in fact they scale with the square of the current density). Therefore, very compact magnets can lead to forces and stresses that damage the superconductor or the insulation. The second aspect is protection: in

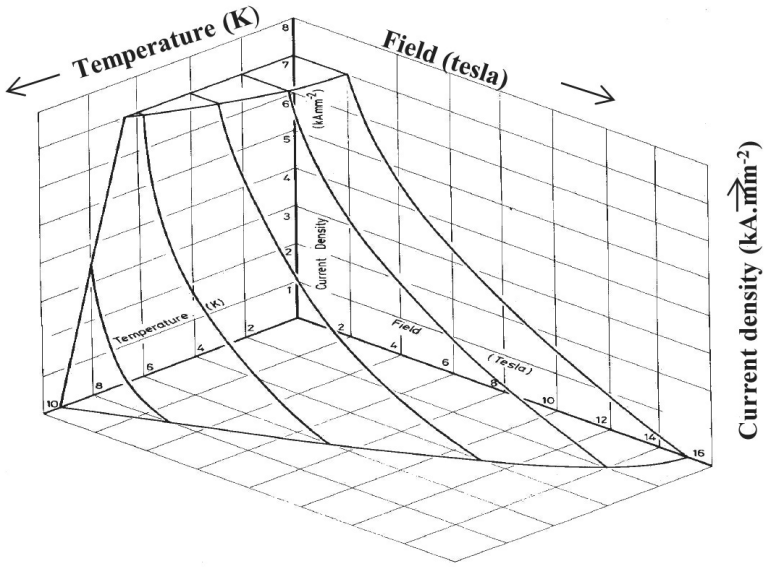

Fig. 5. Sketch of the critical surface of Nb-Ti.

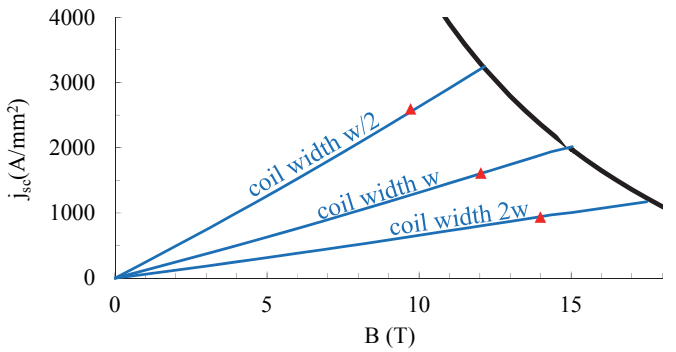

Fig. 6. Cross-section of the critical current versus field for Nb_3Sn at 1.9 K, and loadlines for a coil with width w, $w/2$ and $2w$; red dots indicate operational points with 20% margin.

case of a transition from the superconductive to the resistive state, the energy of the magnetic field has to be dissipated in the coil. A too large energy density brings the coil to an unsafe temperature (usually considered to be above 400 K) or temperature gradient that damages it. So both stress and protection aspects point to avoid current densities in the coil much larger than 500 A/mm^2.

Finally, the design needs to account for production and operation margins. Accelerators magnets usually operate at 50%–80% of the short sample limit, according to the magnet type and technology. Since the operational targets are

usually established before magnet prototyping and production, their selection needs to take into account cost, risk and performance considerations. In the followings, we will carry out the main choices for the HL-LHC magnets: technology, coil width and operational margin.

3.2. *Technology, operational temperature, margin*

In a final focus system, performance is given by large aperture and short length in the region from the interaction point up to the separation dipole. This leads to use in the triplet the Nb_3Sn technology at 1.9 K, which allows doubling the aperture of the present Nb-Ti triplet with a moderate increase of the magnet length (see Fig. 7). In order to maximize performance, a challenging operational point of 80% on the loadline, was selected.

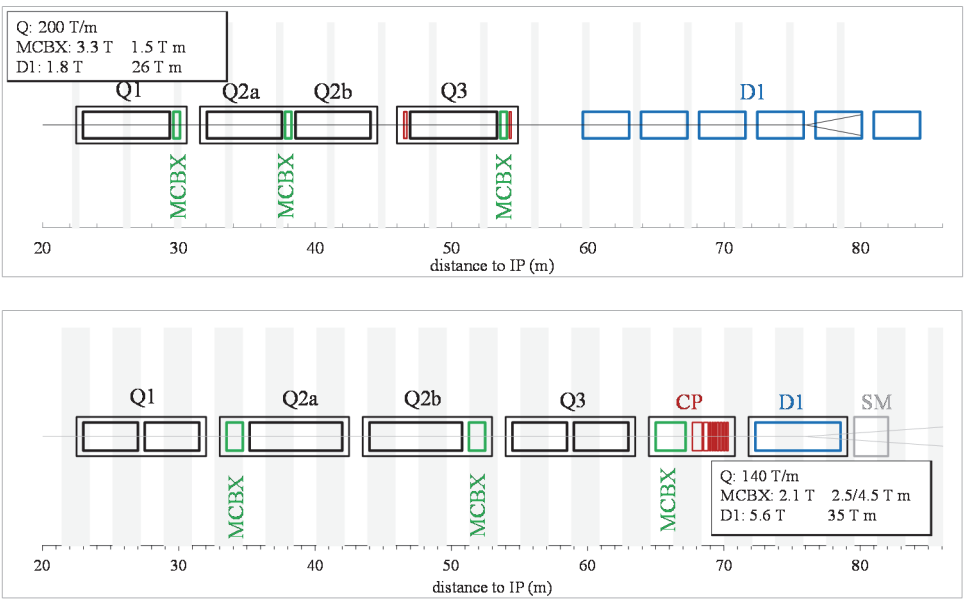

Fig. 7. Lay out of the LHC (upper part) and of HL-LHC (lower part) interaction region from first quadrupole (Q1) to separation dipole (D1).

For the separation/recombination dipole D1 (single aperture), which is presently a resistive magnet (see Fig. 7), we opt for a superconducting magnet with 5.6 T operational field, given by the Nb-Ti technology, with a more conservative operational point of 75% on the loadline [13]. The corresponding reduction in the length of D1 in the upgraded IR more than compensates for the additional space needed by the triplet; in fact, the end of D1 in the HL-LHC layout is 4 meters closer

to the interaction point as compared to the LHC. The option of a Nb_3Sn magnet, considered in the past [14] has been discarded, as the gain of a few meters (3 m, with an 11 T dipole) is not considered critical in this location and has no effect on performance.

The field in the separation/recombination dipole D2 (double aperture) is imposed by field quality constraints. Here the main issue is to reduce the saturation effect. For this reason we chose an operational field of 4.2 T given by the Nb-Ti technology, with a comfortable margin (30%).

The Nb-Ti technology is also chosen for the two-in-one large aperture quadrupole Q4 [15]. With respect to the present baseline, the operational temperature is lowered from 4.5 K to 1.9 K, allowing to better exploit the Nb-Ti performance, with 20% operational margin.

3.3. *Coil width and stress*

For large aperture magnets, stress can become a limiting factor. Values of the order of 200 MPa can damage insulation for Nb-Ti magnets, or degrade conductor performances for the Nb_3Sn magnets. Therefore one has to carefully check in the conceptual design phase that the field and current density values correspond to reasonable values of stress.

For the Nb_3Sn case, in Fig. 8 we plot the operational gradient and the stress versus the coil width. We see that the gain starts to saturate at 30–40 mm, corresponding to a 150 MPa stress, which is large but still within the limits. Going from 35 to 50 mm, i.e. a 50% increase in the superconductor quantity, brings only a 10% increase in gradient. Therefore we chose a ~35 mm width coil width,

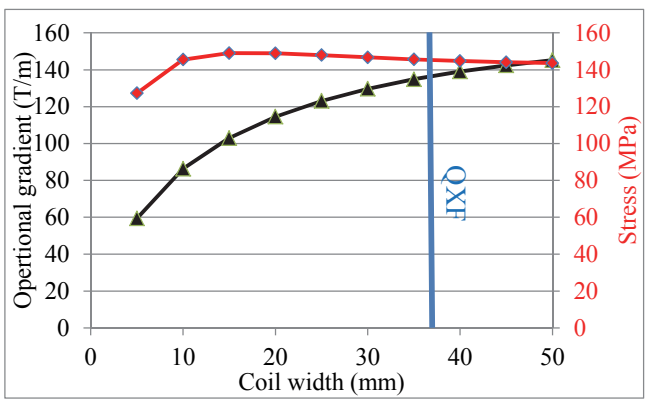

Fig. 8. Operational gradient with 20% margin (black triangles) and stress (red square) versus coil width for 150 mm aperture quadrupole in Nb_3Sn.

providing an operational gradient of ~ 140 T/m. This choice is also related to other factors as previous experience with 90 mm and 120 mm aperture quadrupoles, strand and cable geometry, and quench protection: these aspects will be discussed in the next section.

The present LHC has separation/recombination dipole magnets with a RHIC coil, one layer of 10-mm-wide Nb-Ti cable. We opt for a larger cable, i.e. the LHC main dipole 15-mm-width cable, which has the advantage of having a larger margin and is available in the CERN reserve stock. Choosing a 25% margin on the loadline, we get about 5.6 T and therefore 6.3 m for getting to the 35 T·m requirements. The stress is still manageable at 80 MPa (see Fig. 9). A larger coil width would only marginally reduce the length: two layers with the LHC cable, yielding an effective coil with of 30 mm, would provide 6.5 T (see Fig. 9), i.e. one meter shorter magnets.

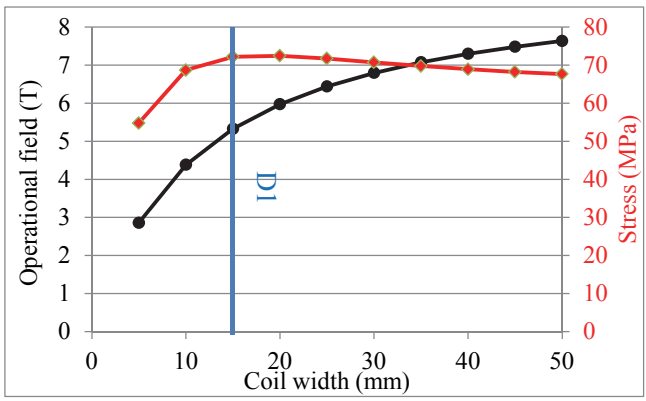

Fig. 9. Operational field with 25% margin (black triangles) and stress (red square) versus coil width for 150 mm aperture dipole in Nb-Ti.

For the D2 we have a preliminary selection of a 15-mm-width cable, a 105 mm aperture, and an operational field of 4 T with a large margin. The main problem of this magnet is a considerable magnetic cross-talk between the apertures.

For the large aperture two-in-one quadrupole Q4, we have a fixed space between the beams, and since we increase the aperture from 70 (present LHC) to 90 mm we have to limit the coil width. We explored possibilities with existing cables developed for the LHC magnets, namely a one layer with 15-mm-width cable, or two layers with 8-mm-width cable. In both cases one has a gradient around 120 T/m (20% loadline margin) with pretty low stress of 50 MPa (see Fig. 10). Doubling the cable width would create a large cross-talk between the apertures, with a modest reduction of the magnet length.

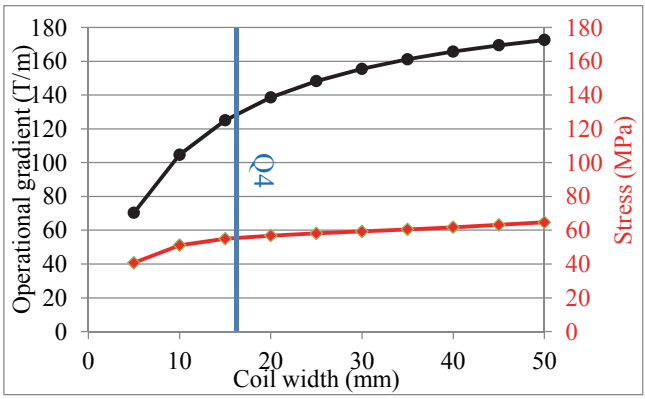

Fig. 10. Operational gradient with 20% margin (black triangles) and stress (red square) versus coil width for 90 mm aperture quadrupole in Nb-Ti.

Table 1. Parameters of the HL-LHC main magnets. Tentative values for orbit corrector and D2 are in italics.

		Triplet Q1,Q3/Q2a,b	Orbit corrector MCBX	Separ. dipole D1	Recomb. dipole D2	Large ap. 2-in-1 Q Q4
Aperture	(mm)	150	150	150	105	90
Field	(T)		*2.1*	5.6	*4.0*	
Gradient	(T/m)	140				120
Mag. Length	(m)	2×4.0/6.8	*1.2/2.2*	6.25	*8.75*	3.5
Int field	(T m)		2.5/4.5	35	35	
Int gradient	(T)	1120/938				420
Peak field	(T)	12.1	*3.5*	6.5	*4.7*	5.9
Current	(kA)	17.5	*2.4*	11.8	*11.7*	16.1
j overall	(A/mm^2)	482	*497*	452	*448*	617
Loadline margin	(%)	20%	*40%*	25%	*40%*	20%
Stored energy	(MJ/m)	1.32	*0.09*	0.338	*0.16*	0.204
Saturation	(%)	9%		12%	*9%*	
Material		Nb_3Sn	Nb-Ti	Nb-Ti	Nb-Ti	Nb-Ti
N. layers		2	*1+1*	1	1	1
N. turns/pole		50	*74*	44	*58*	14
Cable length/pole	(m)	2×450/700	*220/400*	600	*1100*	110
Cable width	(mm)	18.15	*4.37*	15.10	15.10	15.10
Cable thick. in.	(mm)	1.438	0.819	1.362	1.362	1.362
Cable thick. ou.	(mm)	1.612	0.871	1.598	1.598	1.598
Ins. thick rad	(mm)	0.15	0.105	0.13	0.13	0.13
Ins. thick azi	(mm)	0.15	0.105	0.11	0.11	0.11
No. strands		40	18	36	36	36
Strand diam	(mm)	0.85	0.48	0.825	0.825	0.825
Cu/NonCu		1.20	1.75	1.95	1.95	1.95

A summary of the technology, operational field/gradients, peak fields, and loadline margin of the main magnets of the upgrade is given in Table 1.

3.4. *Cryostats and interconnections*

The maximum length of a cryostat that can be lowered in the tunnel is 15 m, corresponding to the main dipole case. Having quadrupoles with lengths ranging from 7 m to 8 m, plus a series of orbit correctors, we are forced to have one cryostat per quadrupole (in LHC Q2a and Q2b share the same cryostat, see Fig. 7). The US LARP collaboration, in charge of the Q1 and Q3 development, has opted for a solution based on having two 4-m-long quadrupole closely connected to form Q1 and Q3 units. This reduces the risk associated to the length, even though it increases costs due to double number of coils and magnet assemblies, and requires doubling manufacturing lines. The Q2 units, under development at CERN, are designed with one 6.8-m-long quadrupole magnet (magnetic length).

We assumed to have 1 m between the cryostats for interconnection. A fine tuning of this length will be carried out during the next stages of the project. Finally, we assumed to have one corrector package and a separation dipole, each one in its cryostat. One could probably merge the two units into a single cryostat, but the gain in performance would be marginal. Also in this case the optimization between performance and risk will take place during the next phases of the project.

3.5. *Cooling*

The cooling of the triplet is provided through heat exchangers. Since the total load on the cold mass is about 15 W/m, one has to use two heat exchangers of 70 mm diameter. The alternative options of one heat exchanger of 110 mm diameter would simplify the interconnections but is not viable since it is not compatible with the magnet mechanical structure. The ideal position for a hole in the yoke of a quadrupole is at 45°, i.e. in the low field region and where less material is needed for structural reasons. An 70 mm heat exchanger is large but still fits the cold mass iron yoke. The short orbit correctors have to share the heat exchanger, i.e. the hole must be in the same positions.

Different options have been considered for the cooling of the corrector package plus the separation dipole, the most effective being another heat exchanger (of 50 mm diameter), this time at 90° from the coil midplane of the dipole.

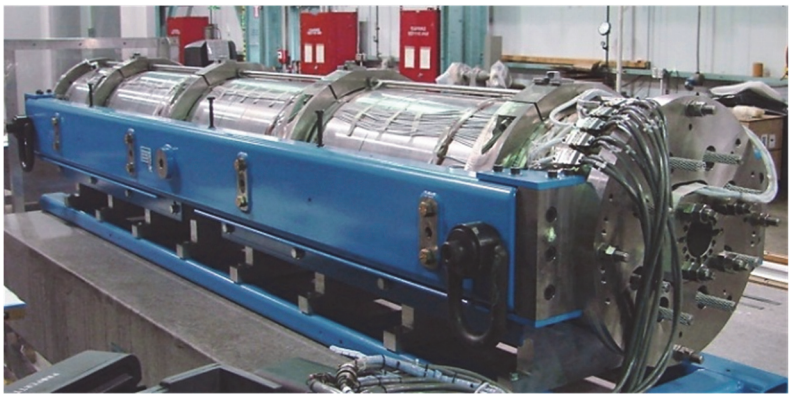

Fig. 11. LQ, the first "long" Nb_3Sn magnet built by LARP collaboration.

4. The Triplet Quadrupoles Q1-Q3

4.1. *Historical development*

The development of Nb_3Sn quadrupoles for the LHC luminosity upgrade was initiated in 2004 by the US LHC Accelerator Research Program (LARP), a collaboration of US National Laboratories and CERN (see Fig. 11). At that time the target was to reach a β^* of 25 cm and a 30% increase of the aperture, from 70 to 90 mm was considered an adequate choice both in terms of machine requirements and technological challenges. After some preliminary tests using racetrack coils, the 1-m-long Technological Quadrupole (TQ) series were developed to address key manufacturing and design issues for $\cos 2\theta$ coils [16]. Two mechanical structures were tested, one based on stainless steel collars and the other on a Al shell pre-loaded using water-pressurized bladders and interference keys [16]. After the test of several models, the bladder and key structure demonstrated a better capability of controlling stress and was selected for the length scale-up from 1 m to 3.4 m (Long Quadrupole (LQ) series), with a first successful test in 2009 (see Fig. 11).

Meanwhile, several works were pointing at the possibility of using apertures larger than 90 mm to increase the upgrade performance [5]. In order to study the feasibility of larger apertures, and demonstrate the capability to incorporate field quality and alignment requirements, in 2008 LARP started the development of the 120-mm-aperture High-field Quadrupole HQ [17]. A successful HQ test at CERN in early 2012 supported a decision to further increase to 150 mm aperture for the triplet quadrupoles (QXF) [19]. The most advanced solutions used in TQ, LQ and HQ are now being applied to the larger aperture quadrupole. So MQXF is

essentially a scaling of the design of HQ [20]. The guideline is to keep all features that have been shown to work properly in the LARP magnets.

4.2. *Strand and cable*

As the aperture in QXF is 25% larger than in HQ, a corresponding increase of the coil width is desirable. In order to minimize deviations from established LARP designs, a two layer coil layout is maintained and the increase in coil width is obtained with an increase in cable width, requiring a larger strand and/or more strands per cable, the option of having one additional layer being excluded to avoid complexity in the coil fabrication. The number of strands is limited by cable mechanical instabilities which affect the winding process, and/or damage to the superconducting strands during the cabling operation. For MQXF, it has been decided to limit the number of strands to 40, which is also the upper limit of the CERN winding machine. A key-stoned cable with 40 strands is already rather difficult to be optimized. TQ cable had 27 strands and 10 mm width, and HQ had 35 strands with 15 mm width. The number of strands and the cable width fixes the strand diameter to 0.85 mm. This is a marginal increase w.r.t. the HQ case, which had 0.8 mm. In all cases we tried to minimize the changes w.r.t. the HQ cases to rely on established design solutions and avoid significant delays to overcome new issues.

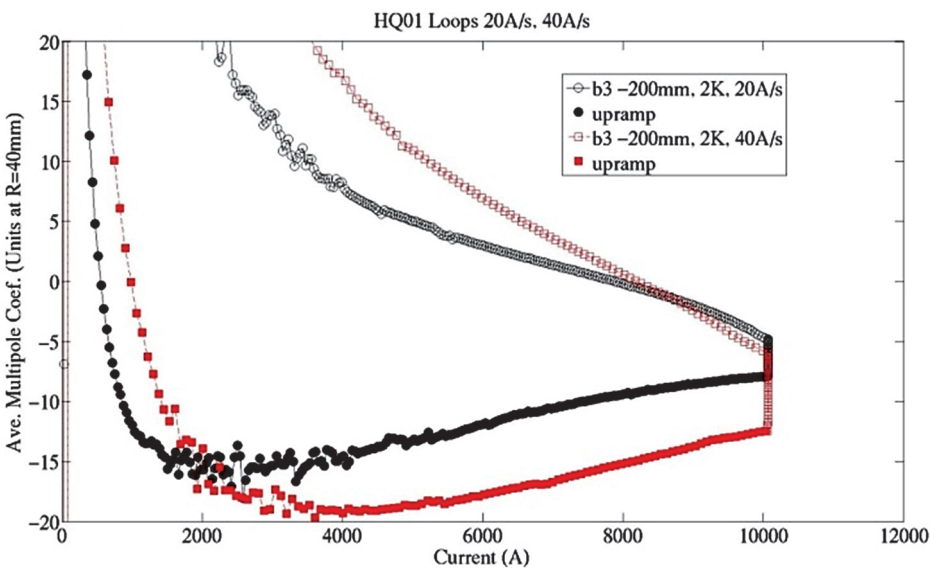

Fig. 12. Dependence of b_3 along the ramp for different ramp rates: case of cable without core (HQ01e).

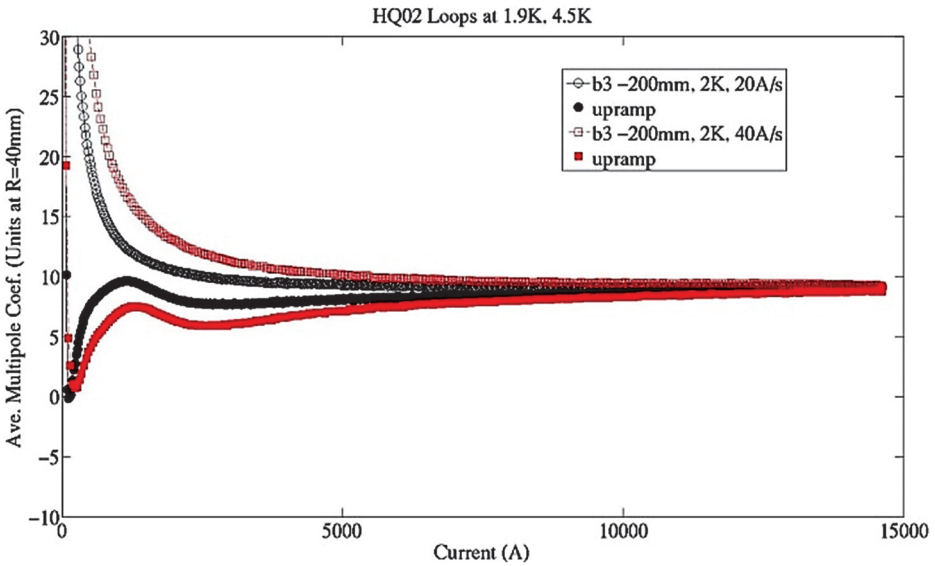

Fig. 13. Dependence of b_3 along the ramp for different ramp rates: case of cable with core (HQ02a).

The other novel aspect is the use of a stainless steel core (25 μm thick) in the cable to increase the inter-strand resistance. Previous LARP quadrupoles, built without cored cables, showed a clear indication of a very low inter-strand resistance (of the order of 0.1–0.5 $\mu\Omega$) [21], producing (i) a severe degradation of quench performance with increasing ramp rate, affecting the capability to perform a fast discharge without quench and (ii) a degradation of field quality, visible as non-allowed components with large dependence on ramp rate, and decay of several units even at high field, with times of the order of a few seconds (see Fig. 12). The second short model HQ02, built with cored cable, proved to cure these issues with an increase of the effective inter-strand resistance by more than one order of magnitude (see Fig. 13).

4.3. *Coil*

The coil is a double layer, four block coil. Two wedges provide the required flexibility to tune the field quality to optimal values. The basic layout of the conductor blocks (Fig. 14) is similar to what has been used in HQ. In particular similar pole angles are chosen for both layers. This approach has been shown to minimize the peak coil stresses. A novel method allowing an exhaustive study of the optimization of the cross-section [22] has shown that the selected option provides a short sample gradient which is very close (less than 1%) to the

maximum gradient attainable with this type of cable (see Fig. 15). In operational conditions the peak field in the coil is 12.2 T, corresponding to a ratio between peak field and gradient times aperture of about 1.15.

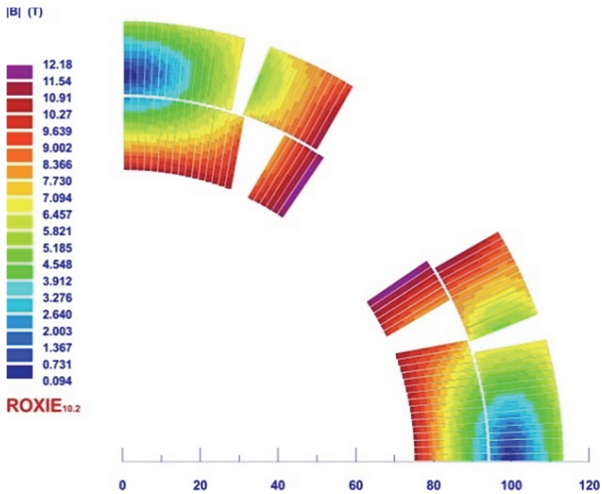

Fig. 14. MQXF coil cross-section (one quarter shown), and field in operational conditions.

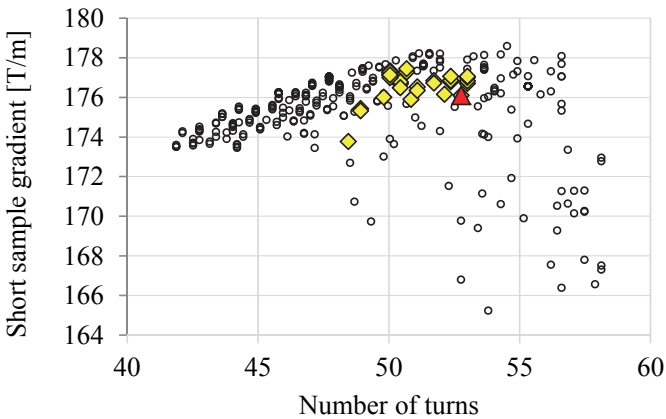

Fig. 15. Short sample gradient provided by 300 different cross-section, satisfying field quality (chosen cross-section: triangle).

4.4. *Mechanical structure*

The Lorentz forces are contained by an aluminium shell (see Fig. 16). During the assembly at room temperature, a prestress of the order of 50 MPa is applied to the coil through the insertion of keys in the slots opened by bladders. During the cool

down, the Al cylinder stress increases to about 150 MPa. This procedure has been used in several models, proving to be an efficient and accurate way to control the stress in the magnet. As the magnet is energized, the pre-load provided by the mechanical structure is replaced by the internal loads generated inside the coils by the electro-magnetic forces (see Fig. 8). Full alignment is maintained at all steps of coil fabrication, magnet assembly and powering. An additional stainless steel vessel is needed for He containment — unfortunately, stainless steel cannot provide the adequate stress increase since its thermal contraction factor is too small, and aluminium cannot provide He containment since it cannot be welded, so two cylinders are needed.

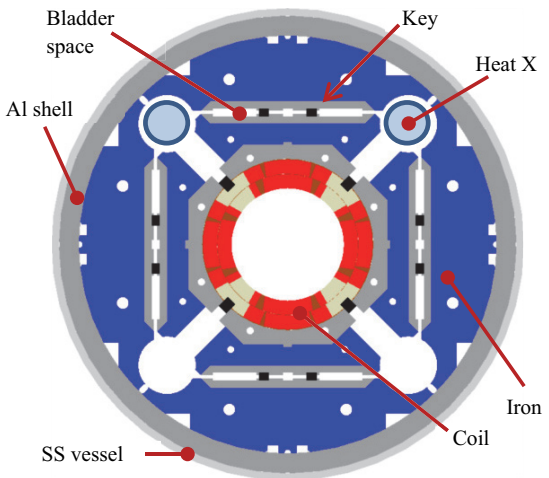

Fig. 16. MQXF cross-section, including heat exchangers.

4.5. *Protection*

The inductance of the QXF magnets is 8–10 mH/m, the lowest value being at nominal current and the highest in the linear regime of non-saturated iron, i.e. at injection. Since the baseline is to have two 8-m-long magnets powered in series, we have an inductance of ~ 0.13 H. The current is 17.5 kA, so the dump resistor is limited to 50 mΩ to avoid having voltages that exceed 900 V at the beginning of the current dump. This means that the time constant of the circuit is of the order of 2 s, and the dump extracts a negligible fraction of the energy stored in the magnetic field. As in the LHC dipoles, the only solution is to use the thermal inertia of the magnet coil to dissipate the energy of the magnetic field. Pending further analysis and verification, a design constraint to remain below ~ 350 K in all points of the coils was adopted.

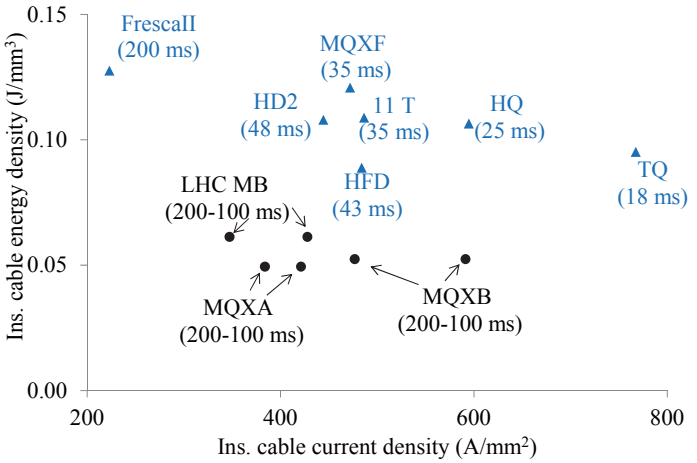

Fig. 17. Snapshot of the protection issues in Nb-Ti and Nb_3Sn magnets: energy density on the coil versus current density, and time margin (circles: Nb-Ti, triangles: Nb_3Sn).

Both Nb-Ti and Nb_3Sn windings have a similar enthalpy from 2 K to 300 K of the order of 0.6 J/mm^3. So the first physical quantity to check is the energy density, i.e. the stored energy divided by the volume of the coil. Note that due to the time scale involved in these phenomena (a fraction of second), the structure components as collars and yoke are too far to share the burden of the heat dissipation — that's why we consider the energy density only over the coil volume. For typical Nb-Ti magnets this value is around 0.05 J/mm^3 (see Fig. 17). In our case, as in many other Nb_3Sn magnets, we are at twice this value, so still well within the enthalpy limit but with half margin.

The key point is to prevent excessive energy dissipation at the initial quench location, which can lead to coil damage due to high local temperature and stress, (hot spot). This requires distributing the energy over the whole magnet, by ensuring rapid transition of the entire winding to the normal conducting state in the fastest possible time. This is done as in most accelerator magnets through quench heaters, i.e. strips of stainless steel which are powered as soon as the quench is detected, and whose heat is transferred via conduction to the coil, pushing it above the critical temperature. The temperature margin in Nb_3Sn is in the range of 5–10 K, the lowest value being reached in the high field zone where the margin on the loadline is 20%. Integrating the specific heats, one finds that has to give 30 μJ/mm^3 in the high field zone. Note that this value is a factor 10 larger w.r.t. to the Nb-Ti case.

A simple way to compare the protection challenge is to compute the time budget (time margin) for the protection system available to quench all magnet, setting 300 K as the maximum temperature reached by the coil [23]. An advantage

of this quantity is that it depends only on the magnet design, and not on the quench features (high field or low field, propagation, etc.) and on the protection system. On the other hand, to make the estimate of the warmest point reached in the magnet (so-called hotspot temperature) one needs other hypothesis on the quench location, efficiency of heaters, propagation, etc.

The time margin is of the order of 100 ms for Nb-Ti magnets (see Fig. 17). In general one needs a few ms to build enough resistance to have a measurable voltage (voltage thresholds are usually set at 100 mV). Then a validation window of 10 ms is used to avoid having false signals. Then the switch of the circuit disconnecting the power converter and dumping the current on the external resistor or on a diode is opened (2 ms). At the same time the heaters are fired. Typical times between the heater firing and the quench of the coil induced by the heaters is 10–20 ms [24] (see Fig. 18).

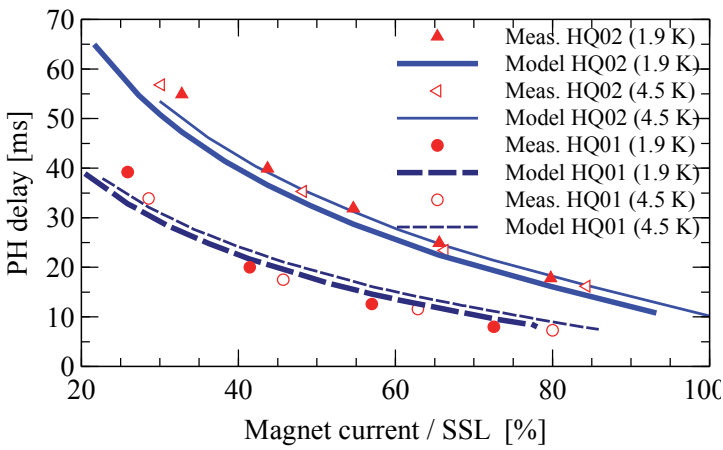

Fig. 18. Quech heater delay versus operational current, in HQ01 and HQ02 featuring 25 and 75 μm thickness of polymide between heatrs and coil.

Therefore, 100 ms seems a comfortable margin, and 50 ms seems a minimal value necessary to have a safe protection system. This time budget is too small in TQ and HQ magnets (15–25 ms). QXF has a larger margin since the current density has been lowered, but it is still on the edge: the present best estimates give about 35 ms.

If one considers heaters on the outer part of the outer layer, protection has to rely on the propagation of the heat from outer to inner layer, which takes of the order of 20 ms. To increase the thin margin, LARP quadrupoles made use of quench heaters on the inner part of the inner layer; these heaters were effective, but in some cases they showed partial detachment after successive quenches.

Moreover they act as a thermal barrier in a region which is critical for heat transfer, so for the triplet one would need a special geometry with gaps. Studies to find an effective solution are ongoing. The present baseline is to have heaters both on the outer part of the outer layer and on 50% of the inner part of the inner layer.

Another possibility is to use quench heaters in the interlayer, but they should be heat treated with the coil, so they would need a completely different technology. A third option is to find ways of making heaters more effective, and/or creating thermal bridges from the outer to the inner layer without endangering the insulation.

4.6. *Field quality and shimming*

When the beams are squeezed in the interaction point, the optical functions in the triplet are very large and the beam dynamics becomes very sensitive to any field imperfection in the triplet. Field quality of the triplet must satisfy tight constraints. The main challenges are (i) a reproducibility of the transfer function of less than one unit (ii) control the low order harmonics within one unit. On the other hand, the nonlinearities coming from the large iron saturation (about 10%, as in HQ, see Fig. 19) can be compensated through an adequate powering of the magnets, provided that the effect is reproducible. Results from the LARP program show that this level of reproducibility is obtained, and that there is a good understanding of the quadrupole main component behavior as a function of the current and of the ramping direction (see Fig. 19).

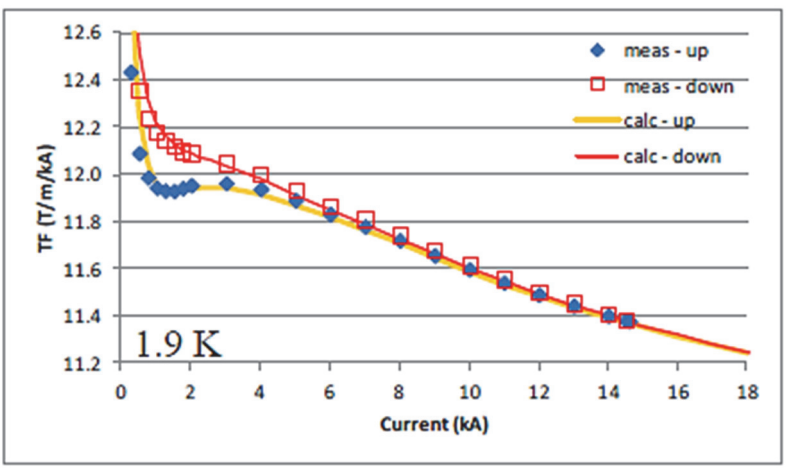

Fig. 19. Ratio between gradient and current for ramping up and down of the quadrupole model HQ.

The low order harmonics are related to the asymmetries of the components and of the assembly. Here, results have not yet shown that the achieved quality is compatible with the beam targets, since in some case several units of non-allowed low-order harmonics (a_3, b_3, a_4, b_4) have been found (see Figs. 12, 13). In principle there is no reason suggesting that Nb_3Sn has a significantly worse field quality for these harmonics (related to asymmetries, i.e. to coil geometry) w.r.t. Nb-Ti. If these effects would persist, a magnetic shimming [25] can be used to compensate for a few large harmonics (typically two at the same time). The technique is based on inserting magnetic rods in holes in the collars and magnetic bars in the spaces used by the bladders. By placing magnetic shims in an asymmetric way, one can compensate up to several units of low order harmonics [26].

Usually a lot of emphasis is put on the first allowed harmonics b_6. In fact, this harmonic is not the most critical for the beam, as it is a high order. Moreover, from the point of view of the magnet builder, it is pretty easy to control b_6 through the cross-section geometry. At injection one has about 20 units given by the magnetizations, which are within the beam dynamics targets.

5. Correctors

5.1. *Orbit correctors*

The beam dynamics requirements for the orbit correctors are 2.5 T·m both in horizontal and vertical plane for the correctors installed next to Q1 and Q2, and 4.5 T·m for the correctors installed next to Q3. This increase in integrated strength is obtained with a corresponding increase in length. The magnets have to operate at any combination of horizontal and vertical field, i.e. a square in the (B_x, B_y) plane. In the LHC we have nested magnets providing 3 T in each plane, with 70 mm aperture. The main challenge of the nested magnet is the management of the large torque (10,000 N·m per meter length of the magnet) coming from the Lorentz forces. In the LHC, this is kept by impregnation — the two layers are "glued" together, and not with a mechanical lock.

For the HL-LHC we consider a nested magnet with an operational field of 2.1 T, giving 1.2 m and 2.1 m magnetic length respectively. With a Rutherford cable composed of 18 strands of 0.45 mm diameter, with a width of 4.5 mm, one can build one-layer coils of a classical $\cos\theta$ layout, reaching 2.1 T with 40% margin. This case ([27], see Fig. 20) has been considered in S-LHC preparatory phase program, set up in the frame of the previous project LHC upgrade phase I, now superseded by HL-LHC. Please note that the peak field is 3.5 T, close to twice the nominal field. This is due to the presence of two perpendicular fields (giving a

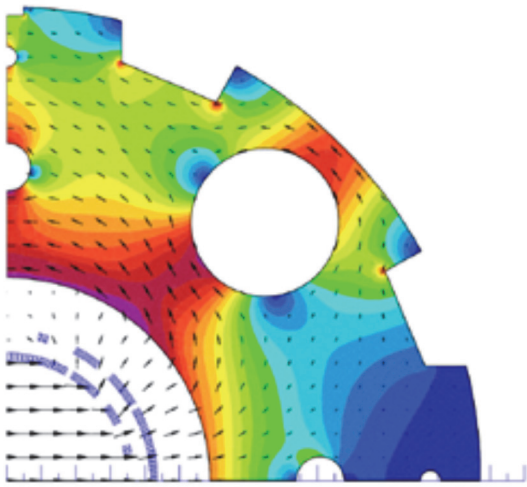

Fig. 20. Cross-section of the orbit correctors developed for SLHC studies (140 mm case [27]).

factor $\sqrt{2}$) plus the ratio coil peak field/bore field, which is ~ 1.3. Large ratios peak field/bore field are unavoidable in dipoles where the coil width is thin with respect to the aperture.

A double layer coils, both for B_x and B_y, would enable reaching ~ 3 T with $\sim 40\%$ margin; this option is also being considered, as it also would allow to make additional room available to the triplet and for the interconnections.

The nested option is challenging from the point of view of the mechanical structure, and to ensure reliability we require that the torque has to be controlled through a mechanical locking. A non-nested option would possibly allow to raise the field, but it would lose the space needed for interconnections and coil ends. Estimating at 100 mm the length of the coil ends per side, and 300 mm for interconnections, the non-nested option gives a 1.5 m longer layout. CIEMAT has taken the responsibility of the magnet design and of the construction of the 1.2-m-long prototype.

5.2. *Linear and nonlinear correctors*

The correction of the triplet imperfections and misalignment requires a large set of correctors. The first requirement is a skew quadrupole, with about 1 T·m integrated force, to correct a tilt in the triplet. Then we have sextupole, octupole, decapole and dodecapole. Requirements for the normal and skew terms are the same, with the exception of the normal b_6, four times larger than a_6 since this is an allowed multipole of the quadrupole and therefore has a larger systematic and random component. The beam dynamics requirements, given in Table 2, are based

on the field error tables of the triplet and of the separation dipole, with an additional safety factor 2 up to order four, and 1.5 for orders five and six. INFN-LASA is in charge of the correctors design and of the construction of prototypes.

In the LHC we have nested correctors, with up to five magnets nested. This solution saves space, but makes operation more complex. For a non-nested solution a key point is to have very short heads, otherwise all the space is lost in heads and interconnections. In the framework of the S-LHC studies, a superferric technology [28] was used to build some prototypes with 140 mm aperture (see Figs. 21 and 22). The magnet has the same cross-section as a resistive magnet, with coils serving to magnetize the iron poles and yoke. In this case, (i) the field quality is given by the shape of the iron poles and not by the precise location of the coils, and (ii) the field is limited at ~ 1.5–2 T due to iron saturation.

Table 2. Parameters of the HL-LHC correctors.

Name	Multipole	Coil length (m)	Force (T m)	Peak field (T)
MCQSX3	a_2	0.716	0.9830	2.20
MCTX3	b_6	0.339	0.0860	2.10
MCTSX3	a_6	0.087	0.0168	2.10
MCDX3	b_5	0.079	0.0254	2.00
MCDSX3	a_5	0.079	0.0254	2.00
MCOX3	b_4	0.137	0.0458	1.25
MCOSX3	a_4	0.137	0.0458	1.25
MCSX3	b_3	0.121	0.0625	1.25
MCSSX3	a_3	0.121	0.0625	1.25

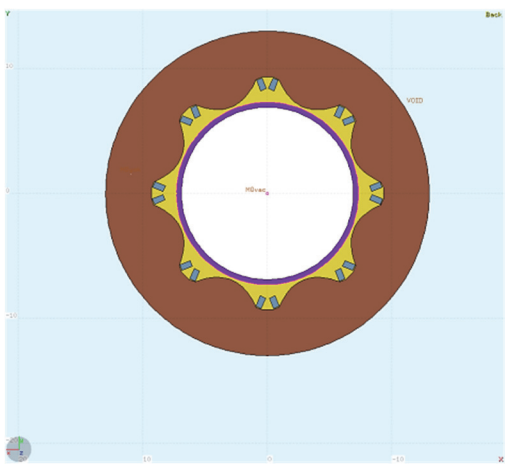

Fig. 21. Superferric correctors cross-section [28].

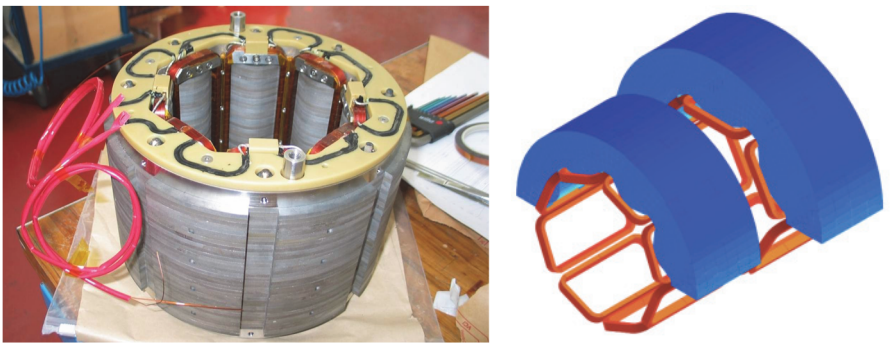

Fig. 22. Superferric correctors [28].

One advantage is that coils are not directly exposed to the aperture, so the magnet is resistant to radiation and additional shielding can be put to protect the coils. The second advantage is that the heads can be made extremely short, with small diameter cable and sharp bends (see Fig. 22), so what is lost in the non-nested option is partially recovered by the shorter heads. It has been also checked that the longitudinal interference between different correctors is negligible even with short interconnection of 80 mm (see Fig. 22, right). The last advantage is that operational current is ~ 100 A, since the conductor is a small single wire. This also simplifies the numerous current leads needed to power this large set of correctors.

This magnet may become a good application for MgB_2 conductor, a novel material characterized by potentially low cost, and current densities vs field properties similar to Nb-Ti. It would be the first application of this conductor to accelerator physics.

6. The Separation Dipole D1

The LHC separation dipole is a 20-m-long resistive magnet, made of 6 modules of 3.4 m length, providing 26 $T \cdot m$ (see Fig. 7). The new specification of integrated field is 35 $T \cdot m$. The replacement of the resistive units with a single Nb-Ti magnet allows recovering the additional space which is needed by the longer triplet. Keeping the same aperture of the triplet, and the same shielding, one can verify that the collision debris induce a heat load and a radiation dose within the project targets. So the replacement of a resistive magnet with a superconductive one is justified.

The main challenges in the magnet design are the large aperture, fringe fields and field quality. The large aperture gives large stored energies and forces, so a proper mechanical structure must be developed. With such a large aperture the

fringe field becomes an issue: with a 5 T operational field in 150 mm aperture, one needs ~ 200 mm of iron to avoid fringe fields. In case of 15 mm coil width and 15 mm spacers, the magnet size reaches $150+(15+15+200)\times 2=610$ in mm diameter, i.e. about the same size of the triplet quadrupole cold mass. This suggest to (i) do not push field to very large values, restricting the study to one-layer coil (ii) have a mechanical structure where forces are taken by the yoke and collars are simple spacers: in this way, more iron is available for shielding.

The baseline is to set the working point at 75% of the loadline, with a Nb-Ti 15-mm-width cable as in the LHC main dipole, providing 5.6 T operational field (see Fig. 23). In this way a 6.3-m-long magnet provides the required 35 $\mathrm{T}\cdot\mathrm{m}$. The iron is largely saturated at nominal field, with a 12% decrease of ratio field/current w.r.t the linear case. Such a large saturation has a relevant impact on field quality, which becomes the main challenge. A careful iron shaping can reduce this effect, following the example of what has been done for the RHIC dipoles [29]. The impact on b_3 can be reduced from the initial values of several tens of units (for a circular iron without holes) to a few units along the operational range (see Fig. 24). Optimization is done at high field. Since there is some uncertainty about the actual energy of the LHC, two cases with 6.5 TeV and 7 TeV have been considered. When choosing the final iron cross-section the energy will be established.

The mechanical structure is similar to the MQXA [30], with support given by the iron yoke locked by keys. This structure has the advantage of reducing the collar size, leaving more space to iron and reducing the fringe field.

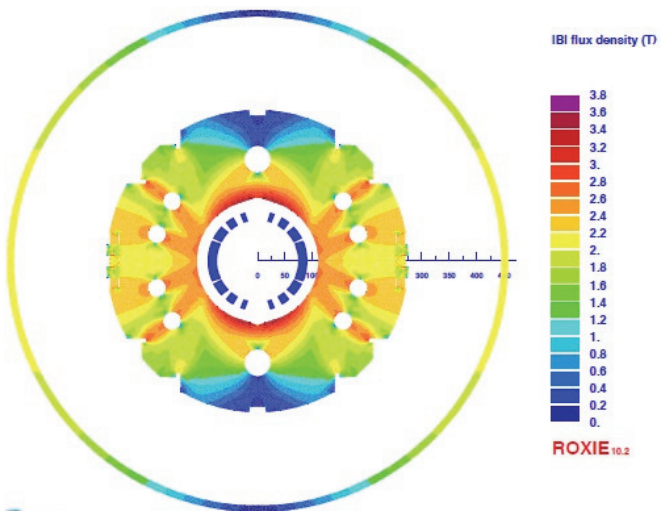

Fig. 23. Cross-section of the separation dipole [13].

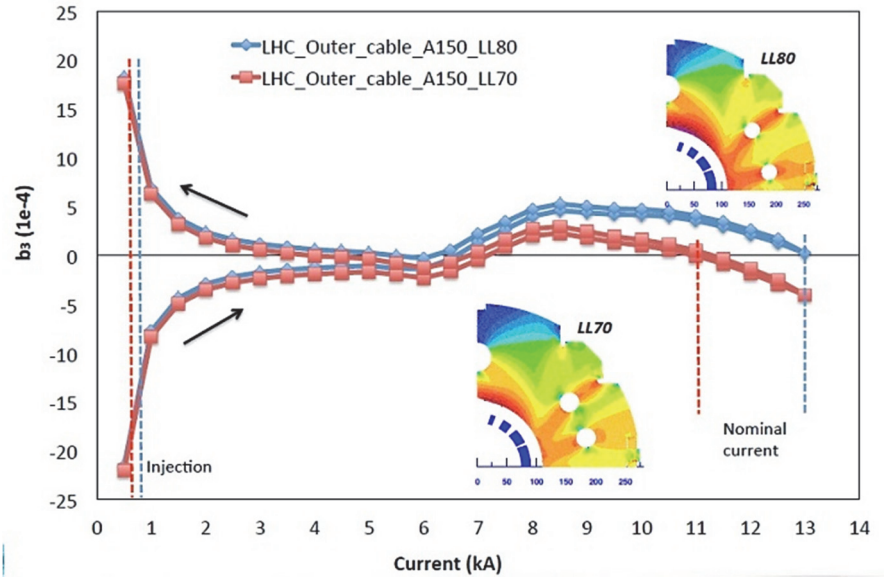

Fig. 24. Cross-section of the separation dipole [13].

7. The Recombination Dipole D2

The recombination dipole needs the same integrated force of 35 T · m to bring the beams back to parallel trajectories, with the nominal spacing of 192 mm. In the LHC this is done by a two-in-one 10-m-long superconducting magnet with ~ 3 T operational field, and 80 mm aperture. Due to the larger beam size one needs to increase this aperture to about 105 mm. In these conditions, since the beam spacing is unchanged, even with a 15-mm thin coil and 15 mm spacing for collars, only a few cm are left between the two apertures, which have the field pointing the same direction. In these conditions, the main design challenge is to decouple the magnetic field in the two apertures and ensure good field quality.

For these reasons, we consider an operational field of 4 T (much lower than D1), giving a magnet length of 9 m. Even with this conservative design choice, using iron yoke as a shield between two apertures leads to unacceptably large saturation effects. Therefore, a different approach was proposed in a study performed by the LARP collaboration [31]: the iron yoke is designed primarily for low saturation effects, and the resulting large but current-independent cross-talk between the apertures is corrected with an asymmetric arrangement of the conductor blocks.

With this approach, it is possible to reach 4 T at 1.9 K with a comfortable 35% margin, and satisfying the field quality requirements. The fringe field on the

cryostat surface is an issue, but can be cured by an oval iron as in the RHIC design. The mechanical structure will also be challenging, since little space is available for collars, a free-standing collar solution (as it adopted for the Q4, see next section) becomes unlikely. So the iron has to support the coil, as in the separation dipole, but in a two-in-one magnet. The design will be performed by INFN-Genova.

8. The Large Aperture Two-in-One Quadrupole

The two-in-one large aperture quadrupole MQY is a 70-mm-aperture magnet with Nb-Ti cable providing 160 T/m at 4.2 K. For the upgrade, the aperture has to be increased to 90 mm. The integrated gradient requirement given by beam dynamics lowers from the LHC baseline of 540 T down to 420 T.

As in the recombination dipole, increasing the aperture with the constraint of the fixed beam separation makes the aperture cross-talk larger, and field quality becomes critical. The case is easier w.r.t the recombination dipole since (i) the magnet is a quadrupole and not a dipole and (ii) one has 15 mm less aperture (see Fig. 25).

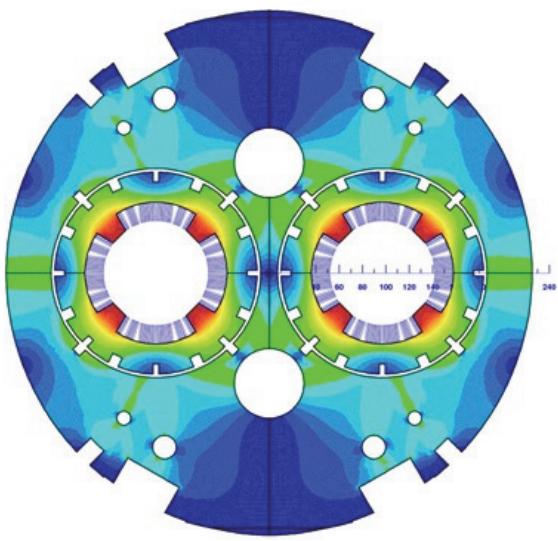

Fig. 25. Cross-section of the large aperture two-in-one quadrupole Q4 [15].

The study has been carried out by CEA-Saclay. Since the integrated gradient requirement is not so large, we decided to have also in this case only 15 mm of coil width. We assume an operational temperature of 1.9 K, as for D2 and crab cavities. Two options were studied, namely a two layer with 8-mm-width cable, and a single

layer with 15-mm-width cable. They both provide 120 T/m with 20% margin on the loadline, and very similar field quality. This would give a 3.5-m-long magnet. With these numbers, it is clear that having a second layer of 15 mm width cable would only marginally increase the gradient (to 160 T/m, see Fig. 10), with a negligible decrease of magnet length, but with much worse field quality.

A 15-mm-thick coil, and the reduced level of forces w.r.t. the recombination dipole, leaves the possibility of having free-standing collars as mechanical structure, with the iron yoke playing only a role for alignment. Field quality can be well optimized.

The baseline is to use the 15-mm-width LHC main dipole cable (outer layer). Since the magnet is short, this can be done with spare cables lengths from the LHC production which could not be used for winding main dipoles. This requires 16 kA operational current, but has the advantage that a dump resistor is enough for the protection, i.e. no quench heaters are needed.

References

[1] O. Brüning *et al.*, LHC luminosity upgrade: a feasibility study, LHC Project Report 626 (2002) 98 p.
[2] J. P. Koutchouk *et al.*, A solution for phase-one upgrade of the LHC low-beta quadrupoles based on Nb-Ti, LHC Project Report 1000 (2007) 23 p.
[3] R. Ostojic *et al.*, Conceptual design of the LHC interaction region upgrade: phase I, LHC Project Report 1163 (2008) 42 p.
[4] J. P. Koutchouk, Investigations of the parameter space for the LHC luminosity upgrade, EPAC (2006) 556–558.
[5] L. Rossi, State of the art superconducting accelerator magnets, *IEEE Trans. Appl. Supercond.* **12**, 219–227 (2002).
[6] L. Rossi, E. Todesco, Electromagnetic design of superconducting quadrupoles, *Phys. Rev. STAB* **9**, 102401 (2006).
[7] N. Mokhov *et al.*, Protecting LHC IP1/IP5 component against radiation resulting from colliding beam interactions, LHC Project Report 633 (2003) 55 p.
[8] V. V. Kashikhin *et al.*, Quench margin measurement in Nb_3Sn quadrupole magnet, *IEEE Trans. Appl. Supercond.* **19**, 2454–2457 (2009).
[9] L. Esposito *et al.*, Fluka energy deposition studies for the HL-LHC, in *IPAC 2013*, 1379–1381.
[10] R. Van Weelderen, Cooling aspects for Nb_3Sn inner triplet quadrupoles and D1, talk on 8th May 2012 given at LARP-Hilumi meeting at FNAL, available at www.cern.ch/hilumi/wp3.
[11] R. Flukiger, T. Spina, The behaviour of copper in view of radiation damage in the LHC luminosity upgrade, CERN Yellow Report 2013-006, 76–82 (2013).
[12] A. Tollestrup *et al.*, The development of superconducting magnets for use in particle accelerators: from Tevatron to the LHC, *Rev. Sci. Accel. Tech.* **1**, 185–210 (2008).

[13] Q. Xu *et al.*, Design optimization of the new D1 dipole for HL-LHC upgrade, *IEEE Trans. Appl. Supercond.* **24**, 4000104 (2014).
[14] A. Den Ouden *et al.*, Progress in the development of an 88-mm bore 10 T Nb_3Sn dipole magnet, *IEEE Trans. Appl. Supercond.* **11**, 2268–2271 (2011).
[15] M. Segreti, J. M. Rifflet, Studies on large aperture Q4, reports I, II and III, (2012–2013), available at http://www.cern.ch/hilumi/wp3.
[16] H. Felice *et al.*, Test results of TQS03: a LARP shell-based Nb3Sn quadrupole using 108/127 conductor, *J. Phys. Conference Series* **234**, 032010 (2010).
[17] F. Borgnolutti *et al.*, Fabrication of a second generation of Nb_3Sn coils for the LARP HQ02 quadrupole magnet, *IEEE Trans. Appl. Supercond.* **24**, 4003005 (2014).
[18] G. Ambrosio *et al.*, Test results and analysis of LQS03 third long Nb_3Sn quadrupole by LARP, *IEEE Trans. Appl. Supercond.* **23**, 4002204 (2013).
[19] E. Todesco *et al.*, A first baseline for the magnets in the high luminosity LHC insertion regions, *IEEE Trans. Appl. Supercond.* **24**, 4003305 (2014).
[20] P. Ferracin *et al.*, Magnet design of the 150 mm aperture low-beta quadrupoles for the high luminosity LHC, *IEEE Trans. Appl. Supercond.* **24**, 4002306 (2014).
[21] X. Wang *et al.*, Multipoles induced by interstrand coupling currents in LARP Nb_3Sn quadrupoles, *IEEE Trans. Appl. Supercond.* **24**, 4002607 (2014).
[22] F. Borgnolutti, Magnetic design optimization of a 150 mm aperture Nb_3Sn low-beta quadrupole for the HiLumi LHC, *IEEE Trans. Appl. Supercond.* **24**, 4000405 (2014).
[23] E. Todesco, Quench limits in the next generation of magnets, CERN Yellow Report 2013-006 (2013) 10–16.
[24] T. Salmi *et al.*, Modeling heat transfer from quench protection heaters to superconducting cables in Nb_3Sn magnets, CERN Yellow Report 2013-006 (2013) 30–37.
[25] R. Gupta, Tuning shims for high field quality in superconducting magnets, *IEEE Trans. Magn.* **32**, 2069–2073 (1996).
[26] P. Hagen, Study of magnetic shimming in triplet magnets, Milestone Report 36 of HiLumi project, available at http://www.cern.ch/hilumi/wp3.
[27] R. Ostojic *et al.*, Conceptual design of the LHC interaction region upgrade: phase I, LHC Project Report 1163 (2008) 14.
[28] F. Toral *et al.*, Development of radiation resistant superconducting corrector magnets for the LHC upgrade, *IEEE Trans. Appl. Supercond.* **23**, 4101204 (2013).
[29] M. Anerella *et al.*, The RHIC magnet system, *Nucl. Instrum. Meths. A* **499**, 280–315 (2003).
[30] Y. Ajima *et al.*, The MQXA quadrupoles for the LHC low-beta insertions, *Nucl. Instrum. Meths. A* **550**, 499–513 (2005).
[31] R. Gupta, G. L. Sabbi, X. Wang, talks given at HiLumi Daresbury meeting (2013), available at https://indico.cern.ch/conferenceDisplay.py?confId=257368.